

University of Texas Rio Grande Valley

ScholarWorks @ UTRGV

Informatics and Engineering Systems Faculty
Publications and Presentations

College of Engineering and Computer Science

5-30-2023

Thermal Transport and Physical Characteristics of Silver-Reinforced Biodegradable Nanolubricant

Jaime Taha-Tijerina

Karla Aviña

Nicolás Antonio Ulloa-Castillo

Dulce Viridiana Melo-Maximo

Follow this and additional works at: https://scholarworks.utrgv.edu/ies_fac



Part of the [Heat Transfer, Combustion Commons](#), [Manufacturing Commons](#), and the [Materials Science and Engineering Commons](#)

Article

Thermal Transport and Physical Characteristics of Silver-Reinforced Biodegradable Nanolubricant

Jose Jaime Taha-Tijerina ^{1,2,*} , Karla Aviña ², Nicolás Antonio Ulloa-Castillo ³ 
and Dulce Viridiana Melo-Maximo ⁴ 

¹ Department of Informatics and Engineering Systems, The University of Texas Rio Grande Valley, Brownsville, TX 78520, USA

² Departamento de Ingeniería, Universidad de Monterrey, Av. Ignacio Morones Prieto 4500 Pte., San Pedro Garza García 66238, Mexico; karla.avina@udem.edu

³ Center for Innovation in Digital Technologies, Department of Mechanical Engineering and Advanced Materials, School of Engineering and Sciences, Tecnológico de Monterrey, Av. Eugenio Garza Sada Sur 2501, Monterrey 64849, Mexico; nicolas.ulloa@tec.mx

⁴ Escuela de Ingeniería y Ciencias, Tecnológico de Monterrey, Mexico City 52926, Mexico; virimelo@tec.mx

* Correspondence: jose.taha@utrgv.edu

Abstract: In this investigation, the thermal transport behavior of biodegradable lubricant reinforced with silver nanostructures (AgNs) at various filler fractions of 0.01, 0.05, 0.10, and 0.20 weight percent was evaluated over a temperature scan analysis, ranging from room temperature up to 60 °C. The experimental results revealed significant gradual enhancements in thermal conductivity as AgNs concentration and evaluating temperatures were increased. These improvements showed the important role of nanostructures' interaction within the biodegradable lubricant. The thermal conductivity performance improved for nanolubricants ranging from 6.5% at 30 °C and 0.20 wt.% AgNs content up to a maximum 32.2%, which was obtained at 60 °C with 0.20 wt.% AgNs concentration. On the other hand, the thermal stability of reinforced lubricants was assessed through thermogravimetric kinetics analyses. The predictive curves resulting from the analyses indicated that there is an enhancement in both the onset temperature for decomposition and the percentage conversion under isothermal conditions for lubricants reinforced with AgNs. Specifically, the results show that the required temperature to achieve a 5% conversion is 100 °C higher than that calculated for bare lubricant. Moreover, the predictive analyses indicate that there is a delay in the decomposition time at isothermal conditions.

Keywords: biodegradable; nanolubricant; thermal transport; thermogravimetric; silver



Citation: Taha-Tijerina, J.J.; Aviña, K.; Ulloa-Castillo, N.A.; Melo-Maximo, D.V. Thermal Transport and Physical Characteristics of Silver-Reinforced Biodegradable Nanolubricant.

Sustainability **2023**, *15*, 8795. <https://doi.org/10.3390/su15118795>

Academic Editor: Pol Torres

Received: 25 April 2023

Revised: 17 May 2023

Accepted: 23 May 2023

Published: 30 May 2023



Copyright: © 2023 by the authors. Licensee MDPI, Basel, Switzerland. This article is an open access article distributed under the terms and conditions of the Creative Commons Attribution (CC BY) license (<https://creativecommons.org/licenses/by/4.0/>).

1. Introduction

Manufacturing processes in numerous industrial sectors have been dealing with important challenges such as cooling and preventive wear or damage of tooling. There has been a considerable amount of developments and investigations focusing on heat-transfer requirements and necessities; however, a major improvement in cooling capability is still insufficient because conventional heat-transfer fluids and lubricants have some limitations in terms of applicability, thermophysical characteristics, and certain restrictions with respect to their working temperature ranges, thermal conductivities, and heat capacities. Additionally, most of these commonly used materials are petroleum-based, which work efficiently for reducing the friction and wear of pair components, diminishing the scuffing of rubbing machinery elements, acting as anti-corrosive protectors, cooling, and other effects. However, these materials are potentially hazardous, having significant ecological impact mainly associated with refineries and increasing issues and concerns for the communities near them. Together with this, attention must be addressed to spillage, material handling by operators, and processes for disposing these petroleum-based lubricants [1–3].

Researchers and industries have focused their efforts to mitigate the environmental health concerns and overcome the effects of the increased pollution affecting every nation and improve the development of sustainable materials and manufacturing processes worldwide. With growing global markets, high demand for efficient, raw material resources management is a key aspect in industrial fields [4]. Particularly, for metal-mechanic manufacturing processes, lubrication and heat dissipation are crucial for product quality and for maintaining low wear or damaging of tooling and equipment [1,2].

Eco-friendly materials have been slowly introduced to counteract the negative contamination effects of petroleum-based lubricants. For instance, water and soil could be affected by spillage or bad disposal of these kinds of materials. Hence, eco-friendly fluids and lubricants are being utilized in sensitive environmental areas [2–5], as they are a good alternative substitute for conventional mineral oils [6,7]. It is also known that biolubricants exhibit inferior performance and higher costs than petroleum-based oils. Nevertheless, recent legal issues and price variations of crude petroleum have provided a niche opportunity for the application of biolubricants, with their own benefits and drawbacks.

Technology and innovation advances in lubricant characteristics and performance have reached a point at which, due to extreme operative conditions such as high temperatures and higher speeds and loads, the materials have been improved by incorporating numerous types of blending additives and reinforcements to conventional fluids and lubricants.

Furthermore, the application of stand-alone biolubricants, regardless of their good characteristics, are limited in thermal transport performance. With the aid of nanotechnology, it is possible to provide a potential enhancement of conventional material properties by incorporating reinforcing nanostructures and developed novel formulated nanolubricants [8–12]. Nanolubricants possess superb characteristics that allow them to be potentially useful in a diverse range of applications. These nanomaterials exhibit enhanced thermal conductivity performance and heat-transfer characteristics as compared to conventional lubricants [13]. Nanolubricants show enhanced stability compared to conventional fluids and lubricants where millimeter- or micrometer-sized particles are incorporated; this results from the size and Brownian motion of the nanostructures within the conventional materials' molecules. Additionally, nanostructures do not easily sediment and wear down the microchannels and pathways in which they flow. Nanolubricants can smoothly flow in a microchannel without clogging, facilitating a possible reduction or miniaturization in the design of the device or systems due to its high heat-transfer efficiency [14,15].

Thermal conductivity as well as physical properties such as viscosity play a significant role in evaluating the quality and efficiency of heat-transfer capacity, which means that fluids and lubricants having enhanced thermal conductivity also possess a good rate of heat transfer. On the other hand, the physico-chemical characteristics of nanolubricants are of relevance to preserve the lubricity and thermal transport. In this sense, lubrication efficiency can be hindered by diverse mechanisms such as contamination, mechanical degradation, thermal degradation, evaporation, and oxidation, among others [16–18]. For example, the oxidation process changes the attributes of fluids and lubricants, leading to a loss of volume and hence a reduction in the lubricant's protective film thickness [19]. Many of such attributes can be investigated through thermal analyses and kinetic studies, which are capable not only of studying thermal processes as thermal decomposition but also of assessing the relevant mechanisms for activation energy in chemical reactions [19–23] and predictive analyses at different conditions through the calculation of kinetic parameters [24–26].

Silver nanostructures (AgNs) are known for their highly antimicrobial properties and are widely employed in commercial products and fields such as healthcare, food storage, and textiles, among others [27–29]. The presence of silver nanostructures can be considered as a reliable alternative for the disinfection of fluids and lubricants from bacteria and pathogens. Corrosion resistance is another characteristic that silver exhibits, which prevents oxidation and the possible degradation of nanostructures. AgNs possess a high surface area per mass, leading to cell lysis and causing the antibacterial effect due to the increased release of silver ions [30,31]. They have gained substantial interest due to their mechanical

attributes such as ductility and low shear strength [32], environmental friendliness [33,34], chemical stability [35,36], thermal transport [34,37,38], and significant potential to enhance the effectiveness of anti-wear performance and friction reduction [27,39–41].

Silver nanostructures reinforcing conventional fluids have been investigated with focus on water as the base material due to its common applications and ubiquity in our environment. However, very few reports are available on silver-based nanofluids or nanolubricants, which have excellent chemical and physical stability, even though this is not widely investigated. The effects of nanosilver content on water-based nanofluids' thermal conductivity was researched by Mirmohammadi et al. [38]. Results showed enhancements in thermal conductivity with the filler fraction increase of nanostructures. For instance, nanofluid at 0.6 vol.% reinforcement showed an improvement in thermal conductivity of about 17% at 293 K and about 26% at 323 K. This behavior was also observed in diverse investigations by Taha-Tijerina et al. [34] and Sunil et al. [42]. Investigations by Godson et al. [43] on the thermal transport behavior of Ag–water nanofluids at various concentrations were performed. They observed an improvement in the heat-transfer coefficient as Ag nanostructures content was increased, reaching an enhancement of 23.5% and 69% at 0.3 and 0.9 vol.%, respectively. The effects of silver nanostructures' size and filler fraction was studied by Paul et al. [44] within conventional water. With a nanostructure size of 55 nm, a maximum improvement of 21% in thermal conductivity was observed. In a similar study, Koca et al. [45] observed an improvement of 11% with 1.0 wt.% of silver concentration within water-based nanofluids, which have potential application in flat-plate solar collectors. Another research by Aberomand et al. [46] described the effects of silver nanostructures on a heat-transfer fluid at different concentrations. A temperature-dependent scanning ranging from 40 °C to 100 °C was performed to evaluate the thermal transport behavior. Results showed a non-linear increase in thermal conductivity as the nanostructures' reinforcing concentration and testing temperature were increased, resulting in the highest performance reaching a maximum improvement of 17% with 0.72 wt.% filler fraction at 100 °C. It was also observed in this research that the enhancement rate of thermal conductivity at lower filler fractions was higher than that displayed at high concentrations. Investigation of silver nanostructures' effect on the thermal transport of ethylene glycol (EG) was performed by Khamliche et al. [47] by comparing to base EG; they experimentally observed an increase of 23% in thermal conductivity with 0.1 vol.% filler fraction at 50 °C. Similarly, Contreras et al. [48] examined the heat-transfer efficiency of Ag–nanofluid, which was composed with 50:50 vol.% of water and EG. Results showed the highest enhancement of 4.7% in heat-transfer rate with 0.05 vol.% filler fraction.

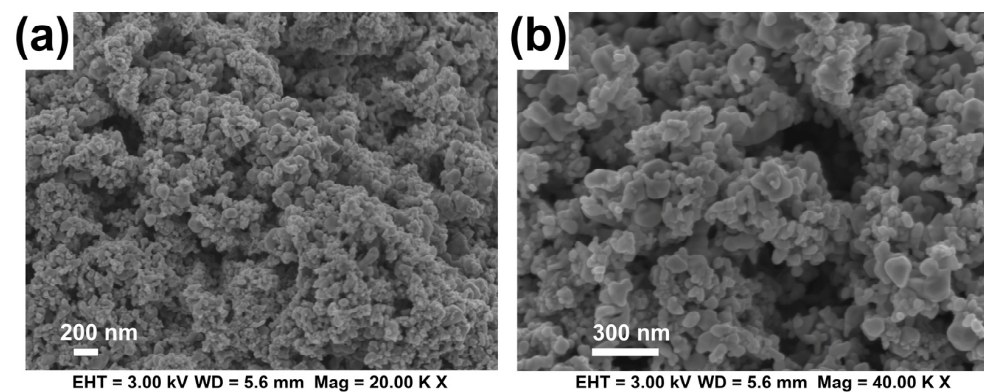
In this study, we propose a biodegradable nanolubricant used for thermal management in diverse industrial applications. The physical and thermal transport characteristics of AgNs nanolubricants at various filler fractions (by weight) were evaluated. The temperature-dependency scans for thermal conductivity evaluations of nanolubricants were measured from room temperature up (24 °C) up to 60 °C, following the transient hot-wire methodology. Furthermore, thermogravimetric analysis was performed to analyze the kinetic thermal degradation according to the Flynn and Wall methodology [49].

2. Materials and Methods

For our research, as the base material, a biodegradable and biostable lubricant, Met-draw CW-D (Servicios Industriales ELSA, S. A. de C. V., Matamoros, Tamaulipas, Mexico), was used (Table 1). Nanolubricants reinforced with sphere-like Ag–nanostructures (AgNs) (Sigma Aldrich Co., St. Louis, MO, USA. CAS#: 7440-22-4) were developed at various filler fractions: 0.01, 0.05, 0.10, and 0.20 wt.%. The morphology and size of AgNs were analyzed with a scanning electron microscope (Carl Zeiss, Sigma VP, New York, NY, USA) (Figure 1). We observed from SEM images the spherical-like shape of the AgNs, which have an average diameter of $54.55 \text{ nm} \pm 19.37 \text{ nm}$ and were measured at 34 nm and 78 nm as the minimum and maximum diameters, respectively.

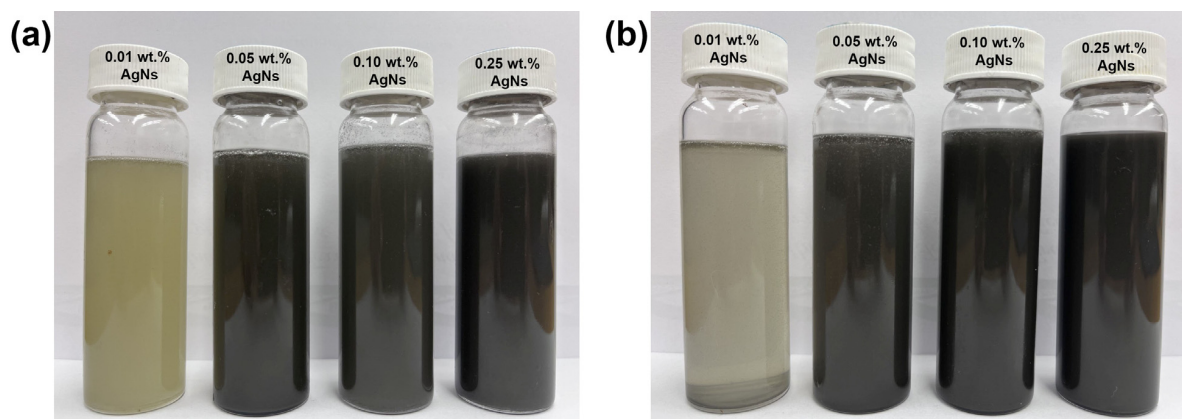
Table 1. Material Characteristics.

Materials		Properties and Characteristics	
Base Lubricant		Density (20 °C)	Kinetic Viscosity (mm ² /s)
Biodegradable oil		0.915 g/cm ³	190 @ 0 °C 32–34 @ 40 °C 7.7–8.3 @ 100 °C
Nanostructures	Properties		
Silver (AgNs)	Morphology: Spherical-like Size-diameter: 54.55 nm ± 19.37 nm Molecular weight: 107.87 g/mol		

**Figure 1.** AgNs morphology at (a) 20 KX and (b) 40 KX magnifications.

Nanolubricants Preparation

Homogeneous dispersions of AgNs within the biodegradable lubricant were prepared following a two-step methodology using a Cole-Parmer 500-Watt probe ultrasonicator for 20 min with 20 kHz at room temperature (24 °C). Various concentrations of nanolubricants were prepared in 120 mL glass containers at 0.01, 0.05, 0.10, and 0.20 weight percent (wt.%). Subsequently, water bath ultrasonication for an extensive time (6–8 h) was employed with a Branson homogenizer (Model 5510—Danbury, CT, USA) and maintaining the water bath at uniform temperature of 24 °C to prevent fast agglomeration of the nanostructures, which could cause quick particle sedimentation and diminished the nanolubricants characteristics. After preparation, the samples were stored in a drawer for 21 days; daily observation of the samples was made, and during this time, samples did not show significant nanostructure sedimentation, as can be observed in Figure 2. Before experimental testing of the nanolubricants, each sample was manually agitated and briefly sonicated for 15 min.

**Figure 2.** AgNs nanolubricant specimens: (a) immediately after extensive water bath sonication and (b) after 3 weeks placed in a drawer.

3. Experimental Details

3.1. Thermal Transport Evaluations

Nanolubricants at diverse AgNs filler fractions were evaluated for thermal conductivity performance following the transient hot-wire method with a thermal analyzer device: TEMPOS (METER GROUP, Inc., Pullman, WA, USA). Thermal conductivity evaluations were performed at various temperatures ranging from room temperature (24 °C) up to 60 °C. For temperatures of 30 °C and above, a water bath was used to maintain a uniform temperature for each of the sample's glass vials. This thermal equilibrium process was used for at least 10 min for each of the samples, producing a homogeneous and uniform temperature in the nanolubricant to then be analyzed. The nanolubricants' effective thermal conductivity (k_{eff}) results were compared with the base biolubricant (k_0). At least eight data measurements were registered for each experiment set, and the average results are reported with error bars as standard deviation.

3.2. Thermogravimetric Analysis (TGA)

A PerkinElmer Pyris 8000 equipment (Mexico City, Mexico) was employed to perform the thermogravimetric analyses. Studies were performed in a temperature range from 50 °C to 650 °C with heating rates of 5, 10, and 15 °C/min. Both nitrogen (N_2) and oxygen (O_2) were used as purge gases during thermal decomposition, and N_2 was used in the temperature range from 30 °C–600 °C and O_2 from 600 °C–650 °C. The kinetic study on thermal degradation was assessed in accordance with the ASTM-E1641-18 standard and using the Flynn and Wall methodology [49], which takes the Arrhenius equation as follows:

$$\left(\frac{d\alpha}{dt}\right) = Z \exp\left(\frac{Ea}{RT}\right)(1 - \alpha)^n \quad (1)$$

where α is the conversion level of decomposition, t is the time (s), Z is the pre-exponential factor (1/s), n is the reaction order ($n = 1$), R is the universal gas constant (8.314 J mol⁻¹ K⁻¹), and Ea is the activation energy (KJ/mol), which was calculated using the following formula.

$$Ea = \frac{-R}{b} \left[\frac{d \log \beta}{d \left(\frac{1}{T}\right)} \right] \quad (2)$$

where T is the temperature at of weight loss, β is the heating rate (°C/min), and b is constant (assuming $n = 1$) [49].

4. Results and Discussion

4.1. Thermal Transport Evaluations

Thermal transport characteristics and attributes (thermal conductivity) are principally governed by the Brownian motion of nanostructures within a fluid or lubricant. In a study by Shafi et al. [50], it was explained how the nanostructures' Brownian motion improved the thermal conductivity performance of a nanolubricant. In the first stage, the nanostructures collide among each other, creating a solid-to-solid heat-transfer conduction mode commonly known as percolation channel formation, followed by a secondary stage in which thermal conduction is increased by a convective heat-transfer mode.

Figure 3 depicts the thermal conductivity results of the experimental measurements of nanolubricants at diverse filler fractions and temperatures. First, it can be observed that the base biolubricant did not show a temperature-dependent behavior, and the thermal conductivity increased only 2.4% at 60 °C compared to the biolubricant at room temperature. Moreover, a progressive enhancement in thermal conductivity was observed with the reinforcing of the concentration and testing temperature increase. For instance, at 30 °C, a slight enhancement in thermal conductivity was displayed. Evaluations at this temperature showed an enhancement of 2.4%, 3.7%, and 4.8% for 0.01, 0.05, and 0.10 wt.%, with a maximum of 6.5% at 0.20 wt.%. However, at 40 °C, the thermal conductivity showed a

more pronounced improvement, ranging from 4.0% at just 0.01 wt.%, 5.4% at 0.05 wt.%, 8.7% at 0.10 wt.%, and up to 11.5% at 0.20 wt.%. Thermal transport enhances gradually as the evaluating temperature rises. Furthermore, at 50 °C, enhancements of 5.6%, 9.1%, and 13.3% were obtained for nanolubricants at 0.01, 0.05, and 0.10 wt.% filler fractions, reaching a maximum increase of 20% at 0.20 wt.% when compared to conventional biolubricant. The chosen evaluating temperatures were selected from previous experimentation work in our research group; they are based on the stabilization of variation of the measurements taken: at higher temperatures, the thermal conductivity measurements present higher error due to the free convection and could be affected due to the circulating water bath, causing forced convection in the samples as well. Finally, when the nanolubricants were evaluated at 60 °C, enhancements of 7.6%, 12.3%, and 20.1% were obtained at 0.01, 0.05, and 0.10 wt.% concentrations, reaching the highest enhancement of 32.2% for the 0.20 wt.% concentration of AgNs compared to pure biolubricant.

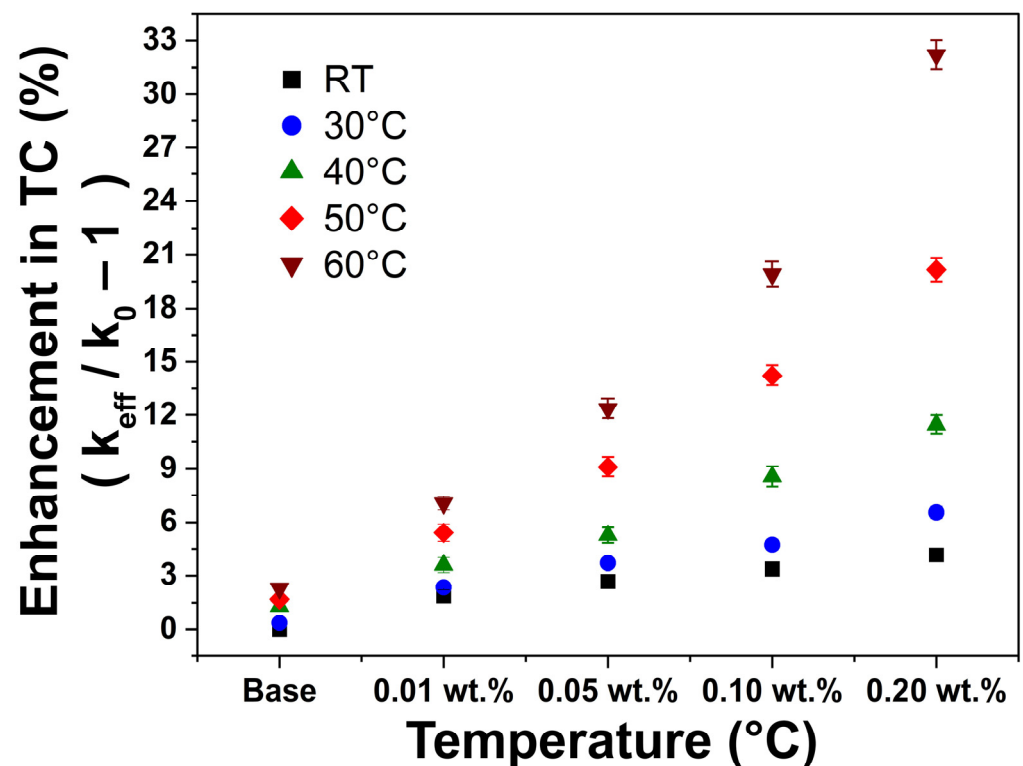


Figure 3. Effective thermal conductivity improvement of nanolubricants at various concentrations based on a temperature-dependent analysis.

These improvements are the result of raising the experimental evaluation temperature and filler fraction of nanostructures, which can be ascribed to the increased Brownian motion velocity, molecular interlayering phenomena, and the surface effects that AgNs can achieve. Additionally, this behavior is attributed to the extensive nanolubricants sonication, in which a molecular layering effect of the lubricant is present. This interfacial layering effect may allow the phonons to much more easily move from one solid nanostructure to another contiguously. This well-organized lubricant layering works as an active thermal transport bridge, allowing more heat transfer across the surface of nanostructures and lubricant molecules and causing the improvement in thermal conductivity [51–53]. As the reinforcing concentration increases, these nanostructures come closer, consequently increasing coherent phonon heat energy distribution within the biodegradable nanolubricant due to Brownian motion.

4.2. Thermogravimetric Analysis

The thermogravimetry curves obtained for all samples are shown in Figure 4a, and their corresponding derivative curve is shown in Figure 4b. Initially, there is a loss of moisture content, and then, thermal degradation occurs in three stages: the first stage can be observed between 140–315 °C, the second stage is observed in the range of 315–420 °C, and finally, the third stage is observed between 420–510 °C. The results show that the products with low molecular weight are eliminated around 350 °C, followed by the degradation of the remaining hydrocarbon at around 400 °C. Finally, the remaining products with higher molecular weight are completely removed above 510 °C.

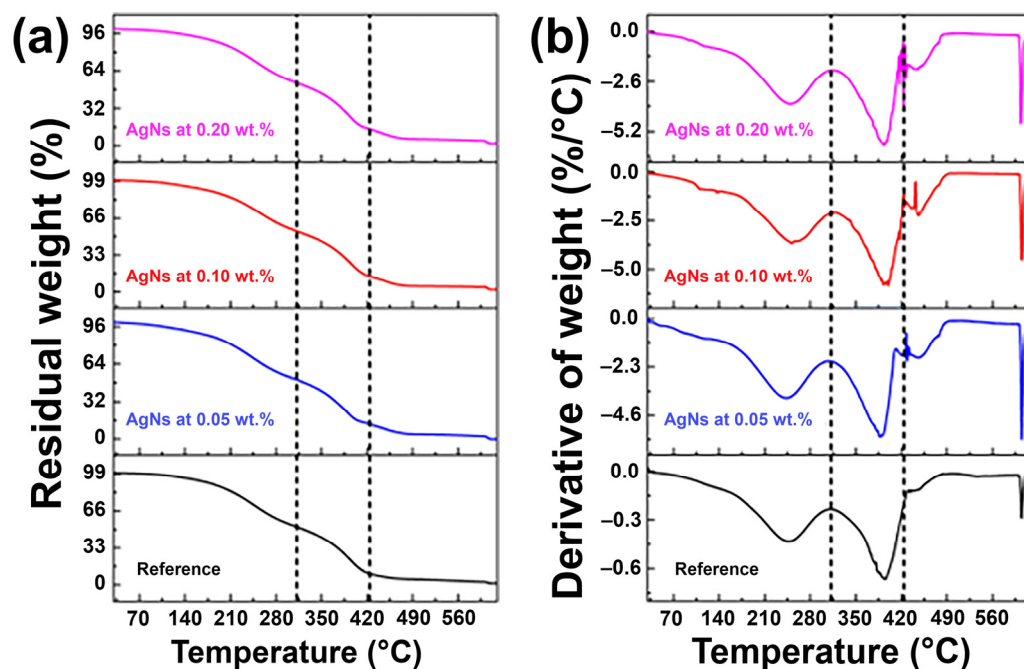


Figure 4. (a) Thermogravimetric curves obtained for nanolubricants reinforced with AgNs at 0.05, 0.10, and 0.20 wt.% and (b) the corresponding derivative curve. Three main steps of degradation are separated by vertical dashed lines.

In general, all samples exhibited the maximum weight loss in the first step of degradation, exhibiting an average loss value of about 47%, while for the second step of degradation, the average weight loss was ~37%. In the third step of degradation, only 3% of weight loss was recorded for the reference sample, while for samples reinforced with AgNs, the average value was 10%. This apparent increase in weight may have originated from heavier molecular products, which require higher temperature for removal. The weight-loss values calculated in each step of degradation are listed in Table 2.

Table 2. Weight loss at different stages (temperatures) and activation energy.

SAMPLE	WEIGHT LOSS (%)			Activation Energy, E_a (KJ/mol)
	First Stage (50 °C–315 °C)	Second Stage (315 °C–420 °C)	Third Stage (420 °C–510 °C)	
Reference	48.2%	43.6%	2.9%	30.7 ± 2.41
AgNs at 0.05 wt.%	49.0%	36.2%	12.2%	25.1 ± 3.17
AgNs at 0.10 wt.%	47.3%	38.8%	9.2%	23.1 ± 3.29
AgNs at 0.20 wt.%	47.2%	37.3%	10.7%	27.7 ± 2.82

A kinetic study on thermal degradation was performed to retrieve the activation energy (E_a) of the reference lubricant sample and nanolubricants at various filler fractions. For the sake of simplicity, Figure 5a,b show only the thermogravimetric curves for the reference and nanolubricant reinforced at 0.10 wt.% of AgNs measured at heating rates of at 5, 10, and 15 °C/min, respectively. Figure 5c shows the Arrhenius plots calculated for all samples, obtaining a steeper slope for the plot obtained for the reference sample, followed by the one obtained for the nanolubricant at 0.20 wt.%, while the ones obtained at 0.05 and 0.10 wt.% were very similar. The latter indicates that the activation energy (E_a) has a higher value for the reference sample (30.7 KJ/mol), while the lowest one was obtained for the nanolubricant at 0.10 wt.% (23.1 KJ/mol). The kinetic parameters retrieved from the TGA data assisted with the kinetic software from PerkinElmer and are shown in Table 2.

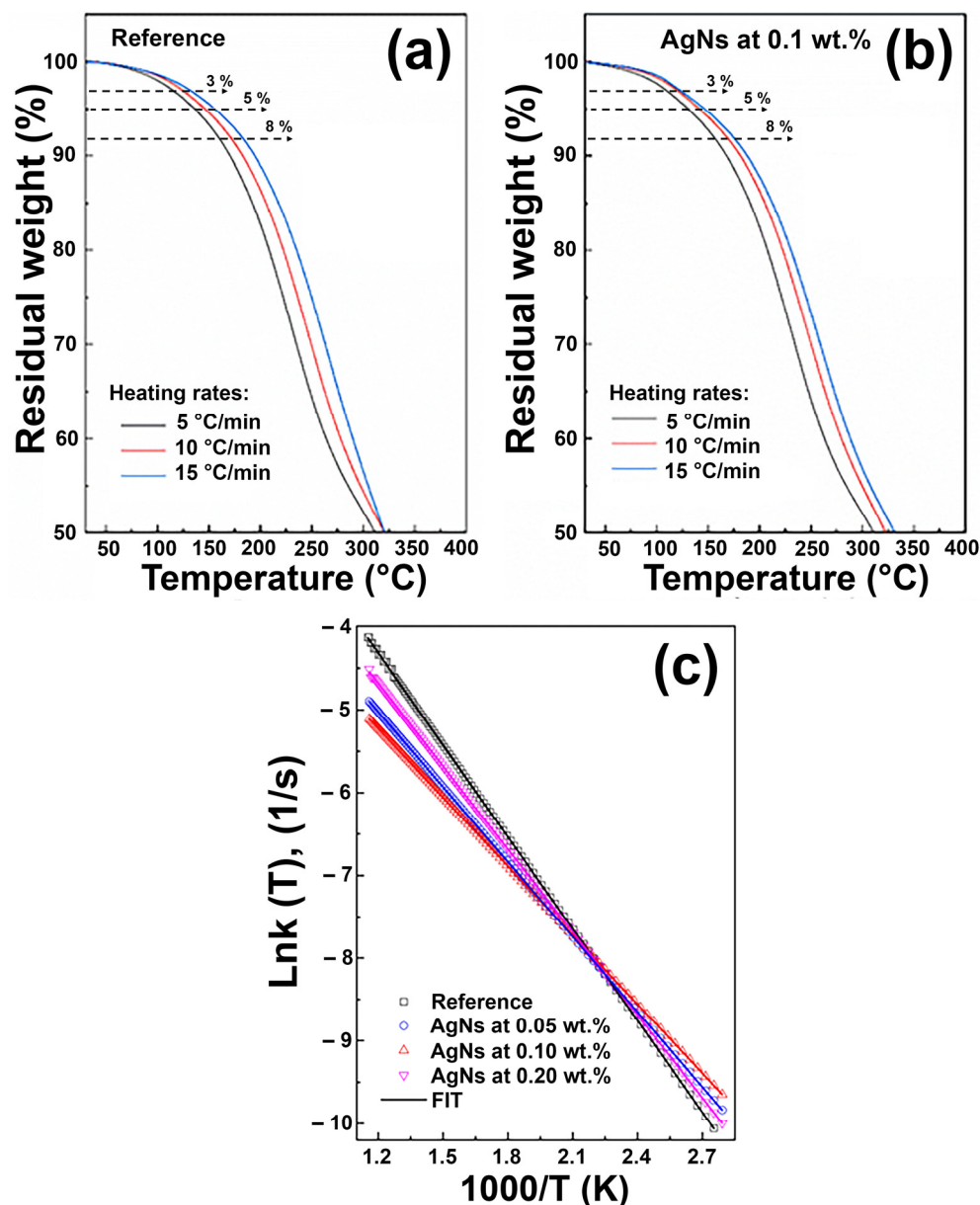


Figure 5. Thermogravimetric curves of (a) reference sample and (b) nanolubricant reinforced at 0.10 wt.% AgNs, measured at 5, 10, and 15 °C/min heating rates. (c) Arrhenius plots calculated for the reference lubricant and the nanolubricants.

The predictive curves resulting from the kinetic analyses are shown in Figure 6. The required temperature to achieve a 5% conversion level at various holding times is depicted in Figure 6a–d. The analyses show that the onset temperature for decomposition increases (indicated by the orange arrow) for samples reinforced with AgNs such that the conversion for bare lubricant is completed at 420 °C, while for nanolubricants, this takes place at 520 °C, 550 °C, and 470 °C at 0.05, 0.10, and 0.20 wt.% of AgNs, respectively. On the other hand, the corresponding analyses for percentage conversion under isothermal conditions are depicted in Figure 6e–h. The results indicate that the thermal decomposition reaction for nanolubricants is significantly slower than for the bare reference sample. For instance, in the temperature range from 300 °C to 400 °C, the decomposition for bare lubricant is completed within the 55 min of reaction, while the nanolubricants exhibit resistance to decomposition until 87 min, 89 min, and 71 min at 0.05, 0.10, and 0.20 wt.% of AgNs, respectively. It is possible to note that the predicted values for sample at 0.20 wt.% are lower than those obtained for the nanolubricants at 0.05 and 0.10 wt.% of AgNs. This is an expected result since the activation energy at 0.20 wt.% is very similar to the bare lubricant, suggesting that thermal stability may be affected at higher filler concentrations.

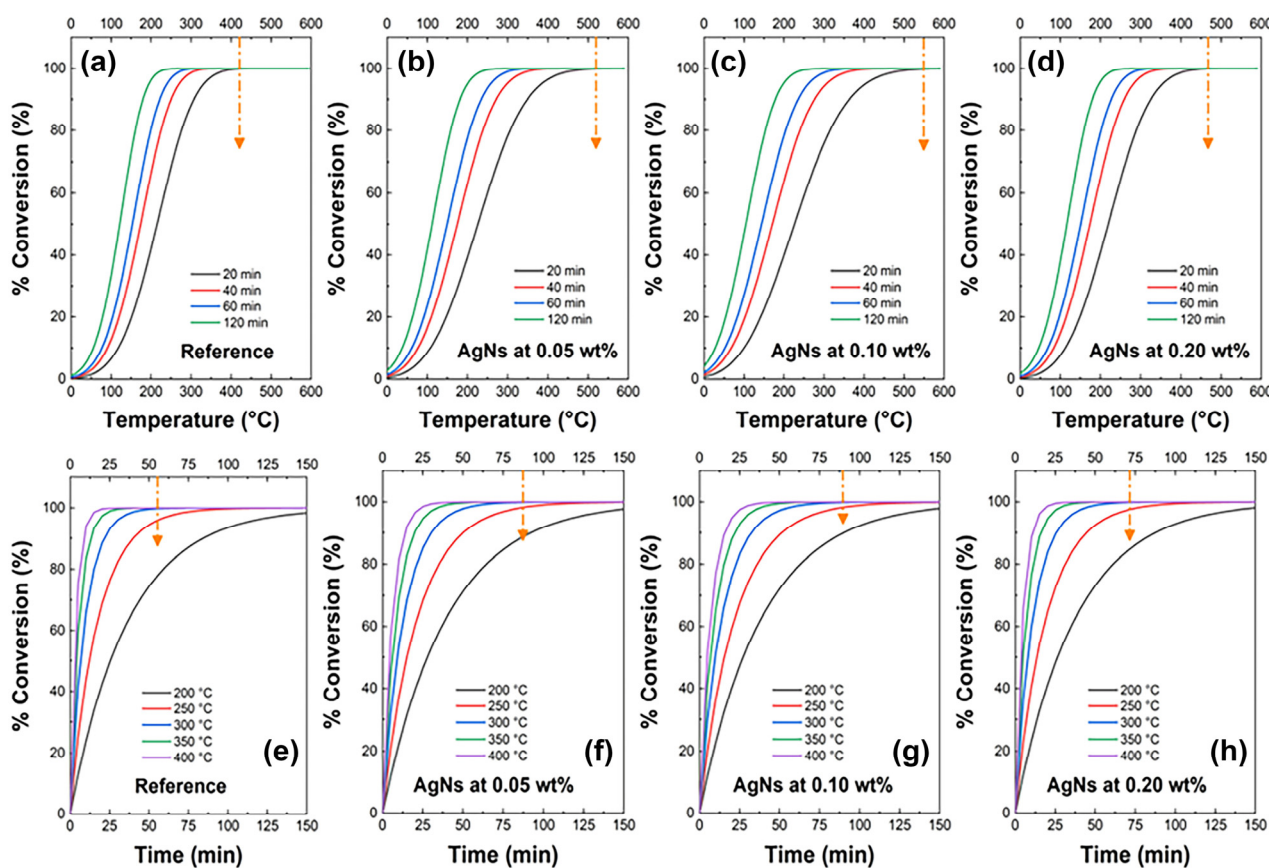


Figure 6. Predictive decomposition curves under (a–d) isochronal and (e–h) isothermal conditions retrieved for bare lubricant and nanolubricants reinforced at 0.05, 0.10, and 0.20 wt.% of AgNs. Dashed lines indicate complete conversion.

It is of relevance to mention that there is a slightly higher onset temperature for decomposition for the nanolubricants, indicating that there is an enhancement of thermal properties due to the incorporation of AgNs within the biolubricant reference sample. The latter indicates that the AgNs provide thermal stability to the biolubricant such that the decomposition reaction occurs more slowly than for the biolubricant base.

5. Conclusions

Ecofriendly fluids and lubricants are a novel type of materials engineered and developed to address concerns about the environmental impact of traditional petroleum-based fluids and lubricants. Improving environmental awareness is a crucial driving force to continue developing new technologies and innovations such as the usage of biodegradable materials in environmentally sensitive areas, which are needed in diverse fields and industrial applications. In this work, a biodegradable lubricant was reinforced with silver nanostructures at various filler fractions. Evaluation of the nanolubricants at diverse temperatures was performed to determine its effect on thermal transport behavior. These environmentally friendly nanolubricants showed positive results and good potential as alternative materials for industrial applications where heat dissipation plays a critical role. The thermal transport behavior was greatly affected by chemical and physical characteristics of the conventional biolubricant as well as the interactions among the reinforcing nanostructures and biolubricants molecules.

In general, nanolubricants demonstrated a temperature dependency in their thermal conductivity performance, indicating the important role of the nanostructure's interaction within the biodegradable lubricant. From measurements at room temperature up to 60 °C, increasing filler fraction showed a significant enhancement in thermal conductivity, achieving significant enhancements ranging from 6.5% at 30 °C and 0.20 wt.% up to a maximum 32.2% obtained at 60 °C with 0.20 wt.% AgNs concentration. This improvement in thermal transport behavior as a function of increasing evaluation temperature and AgNs concentration indicates the contribution of Brownian motion. At higher temperatures, Brownian velocity is increased, and it is also suggested that this effect is attributed to the interactions among the nanostructures and biolubricant molecules. Another important aspect is that at higher AgNs concentrations, a percolative-like improvement of the thermal conductivity of nanolubricants due to the direct heat transport via AgNs colliding can be triggered. Furthermore, the development of thermal bridges among biolubricant and AgNs can also be a potential cause for the enhancement of thermal conductivity.

The thermogravimetric analyses exhibited three decomposition stages, obtaining the maximum weight loss (~47%) in the first degradation step (50–300 °C). Activation energy values (E_a) for decomposition were retrieved from TGA kinetics analyses, obtaining lower values for the nanolubricant reinforced with AgNs at 0.10 wt.% (~23 KJ/mol) than for the biolubricant reference (~30 KJ/mol). With the thermogravimetric analysis performed and results achieved, it is suggested that the AgNs provide thermal stability to the lubricant such that the decomposition reaction occurs more slowly.

Author Contributions: Conceptualization, J.J.T.-T. and N.A.U.-C.; methodology, J.J.T.-T. and N.A.U.-C.; validation, J.J.T.-T., K.A., D.V.M.-M. and N.A.U.-C.; formal analysis, J.J.T.-T. and N.A.U.-C.; investigation, J.J.T.-T., K.A., D.V.M.-M. and N.A.U.-C.; resources, J.J.T.-T. and N.A.U.-C.; data curation, J.J.T.-T., K.A. and N.A.U.-C.; writing—original draft preparation, J.J.T.-T. and N.A.U.-C.; writing—review and editing, J.J.T.-T., K.A., D.V.M.-M. and N.A.U.-C.; visualization, J.J.T.-T. and N.A.U.-C.; supervision, J.J.T.-T. and N.A.U.-C.; project administration, J.J.T.-T. All authors have read and agreed to the published version of the manuscript.

Funding: This research received no external funding.

Institutional Review Board Statement: Not applicable.

Informed Consent Statement: Not applicable.

Data Availability Statement: Not applicable.

Acknowledgments: Authors acknowledge the support from ELSA Lubricantes and Julio Castillo for supplying the biodegradable lubricant for this work.

Conflicts of Interest: The authors declare no conflict of interest.

References

1. Diabb-Zavala, J.M.; Martínez-Romero, O.; Elías-Zúñiga, A.; Leija-Gutiérrez, H.M.; Estrada-De La Vega, A.; Taha-Tijerina, J. Study of Friction and Wear Effects in Aluminum Parts Manufactured via Single Point Incremental Forming Process Using Petroleum and Vegetable Oil-Based Lubricants. *Materials* **2021**, *14*, 3973. [[CrossRef](#)] [[PubMed](#)]
2. Krolczyk, G.M.; Maruda, R.W.; Krolczyk, J.B.; Wojciechowski, S.; Mia, M.; Nieslony, P. Ecological trends in machining as a key factor in sustainable production—A review. *J. Clean. Prod.* **2019**, *218*, 601–615. [[CrossRef](#)]
3. Elsaid, K.; Olabi, A.G.; Wilberforce, T.; Abdelkareem, M.A.; Sayed, E.T. Environmental impacts of nanofluids: A review. *Sci. Total Environ.* **2021**, *763*, 144202. [[CrossRef](#)] [[PubMed](#)]
4. Kazeem, R.A.; Fadare, D.A.; Ikumapayi, O.M.; Adediran, A.A.; Aliyu, S.J.; Akinlabi, S.A. Advances in the Application of Vegetable-Oil-Based Cutting Fluids to Sustainable Machining Operations: A Review. *Lubricants* **2022**, *10*, 69. [[CrossRef](#)]
5. Rani, S.; Joy, M.L.; Nair, K.P. Evaluation of physiochemical and tribological properties of rice bran oil—Biodegradable and potential base stock for industrial lubricants. *Ind. Crops Prod.* **2015**, *65*, 328–333. [[CrossRef](#)]
6. Ahmad, U.; Naqvi, S.R.; Ali, I.; Naqvi, M.; Asif, S.; Bokhari, A. A review on properties, challenges and commercial aspects of eco-friendly biolubricants productions. *Chemosphere* **2022**, *309*, 136622. [[CrossRef](#)] [[PubMed](#)]
7. Uppar, R.; Dinesha, P.; Kumar, S. A critical review on vegetable oil-based bio-lubricants: Preparation, characterization, and challenges. *Environ. Dev. Sustain.* **2022**, 1–36. [[CrossRef](#)]
8. Taha-Tijerina, J.J.; Martínez, J.M.; Eustest, D.; Arqueta-Guillén, P.Y. Carbon Nanotube Reinforced Lubricants in Plastic Deformation Processes. *Lubricants* **2022**, *10*, 74. [[CrossRef](#)]
9. Taha-Tijerina, J.; Aviña, K.; Diabb, J.M. Tribological and thermal transport performance of SiO₂-based natural lubricants. *Lubricants* **2019**, *7*, 71. [[CrossRef](#)]
10. Wu, H.; Kamali, H.; Huo, M.; Lin, F.; Huang, S.; Huang, H. Eco-Friendly Water-Based Nanolubricants for Industrial-Scale Hot Steel Rolling. *Lubricants* **2020**, *8*, 96. [[CrossRef](#)]
11. Morshed, A.; Wu, H.; Jiang, Z. A Comprehensive Review of Water-Based Nanolubricants. *Lubricants* **2021**, *9*, 89. [[CrossRef](#)]
12. Roy, S.; Zhang, X.; Puthirath, A.B.; Meiyazhagan, A.; Bhattacharyya, S.; Rahman, M.M.; Taha-Tijerina, J.J. Structure, Properties and Applications of Two-Dimensional Hexagonal Boron Nitride. *Adv. Mater.* **2021**, *33*, 2101589. [[CrossRef](#)]
13. Suresh, K.; Selvakumar, P.; Kumaresan, G.; Vijayakumar, M.; Ravikumar, M.; Jenita, N.R. A critical review on the effect of morphology, stability, and thermophysical properties of graphene nanoparticles in nanolubricants and nanofluids. *J. Therm. Anal. Calorim.* **2022**, *148*, 451–472. [[CrossRef](#)]
14. Apmann, K.; Fulmer, R.; Scherer, B.; Good, S.; Wohld, J.; Vafaei, S. Nanofluid Heat Transfer: Enhancement of the Heat Transfer Coefficient inside Microchannels. *Nanomaterials* **2022**, *12*, 615. [[CrossRef](#)] [[PubMed](#)]
15. Bhattacharyya, S.; Abro, K.A.; Souayah, B.; Yasmin, H.; Giwa, S.O.; Noor, S. Reproduction of Nanofluid Synthesis, Thermal Properties and Experiments in Engineering: A Research Paradigm Shift. *Energies* **2023**, *16*, 1145.
16. Ito, H.; Tomaru, M.; Suzuki, T. Physical and chemical aspects of grease deterioration in sealed ball bearings. *Lubr. Eng.* **1988**, *44*, 872–879.
17. Mustafa, W.A.A.; Dassenoy, F.; Sarno, M.; Senatore, A. A review on potentials and challenges of nanolubricants as promising lubricants for electric vehicles. *Lubr. Sci.* **2022**, *34*, 1–29. [[CrossRef](#)]
18. Ali, M.K.A.; Xianjun, H. Improving the heat transfer capability and thermal stability of vehicle engine oils using Al₂O₃/TiO₂ nanomaterials. *Powder Technol.* **2020**, *363*, 48–58. [[CrossRef](#)]
19. Smook, L.A.; Sathwik, S.C.; Lugt, P.M. Evaluating the oxidation properties of lubricants via non-isothermal thermogravimetric analysis: Estimating induction times and oxidation stability. *Tribol. Int.* **2022**, *171*, 107569. [[CrossRef](#)]
20. Dos Santos-Politi, J.R.; De Matos, P.R.R.; Sales, M.J.A. Comparative study of the oxidative and thermal stability of vegetable oils to be used as lubricant bases. *J. Therm. Anal. Calorim.* **2013**, *111*, 1437–1442. [[CrossRef](#)]
21. Khan, U.; Zaib, A.; Ishak, A. Impact of Thermal and Activation Energies on Glauert Wall Jet (WJ) Heat and Mass Transfer Flows Induced by ZnO-SAE50 Nano Lubricants with Chemical Reaction: The Case of Brinkman-Extended Darcy Model. *Lubricants* **2023**, *11*, 22. [[CrossRef](#)]
22. Lugt, P.M. Grease Aging. In *Grease Lubrication in Rolling Bearings*; John Wiley and Sons: Hoboken, NJ, USA, 2012; pp. 171–190.
23. Fasehullah, M.; Wang, F.; Jamil, S.; Bhutta, M.S. Influence of Emerging Semiconductive Nanoparticles on AC Dielectric Strength of Synthetic Ester Midel-7131 Insulating Oil. *Materials* **2022**, *15*, 4689. [[CrossRef](#)] [[PubMed](#)]
24. Wan-Nik, W.B.; Ani, F.N.; Masjuki, H.H. Thermal stability evaluation of palm oil as energy transport media. *Energy Convers. Manag.* **2005**, *46*, 2198–2215. [[CrossRef](#)]
25. López, T.D.-F.; González, A.F.; Del Reguero, Á.; Matos, M.; Díaz-García, M.E.; Badía-Laíño, R. Engineered silica nanoparticles as additives in lubricant oils. *Sci. Technol. Adv. Mater.* **2015**, *16*, 055005. [[CrossRef](#)] [[PubMed](#)]
26. Rasheed, A.K.; Khalid, M.; Javeed, A.; Rashmi, W.; Gupta, T.C.S.M.; Chan, A. Heat transfer and tribological performance of graphene nanolubricant in an internal combustion engine. *Tribol. Int.* **2016**, *103*, 504–515. [[CrossRef](#)]
27. Ghaednia, H.; Hossain, M.S.; Jackson, R.L. Tribological Performance of Silver Nanoparticle-Enhanced Polyethylene Glycol Lubricants. *Tribol. Trans.* **2015**, *59*, 585–592. [[CrossRef](#)]
28. Naganthran, A.; Verasoundarapandian, G.; Khalid, F.E.; Masarudin, M.J.; Zulharnain, A.; Nawawi, N.M. Synthesis, Characterization and Biomedical Application of Silver Nanoparticles. *Materials* **2022**, *15*, 427. [[CrossRef](#)]
29. Salata, O.V. Applications of nanoparticles in biology and medicine. *J. Nanobiotechnol.* **2004**, *2*, 3. [[CrossRef](#)]

30. Tripathi, N.; Goshisht, M.K. Recent Advances and Mechanistic Insights into Antibacterial Activity, Antibiofilm Activity, and Cytotoxicity of Silver Nanoparticles. *ACS Appl. Bio. Mater.* **2022**, *5*, 1391–1463. [[CrossRef](#)]
31. Zhang, Z.; Shen, W.; Xue, J.; Liu, Y.; Liu, Y.; Yan, P. Recent advances in synthetic methods and applications of silver nanostructures. *Nanoscale Res. Lett.* **2018**, *13*, 54. [[CrossRef](#)]
32. Du, F.; Li, C.; Li, D.; Sa, X.; Yu, Y.; Li, C. Research Progress Regarding the Use of Metal and Metal Oxide Nanoparticles as Lubricant Additives. *Lubricants* **2022**, *10*, 196. [[CrossRef](#)]
33. Chinnachamy, R.; Durairaj, V.; Saravanamuthu, M.; Rajagopal, V. Evaluation of the effect of silver nanoparticles on the tribological and thermophysical properties of bio-lubricants. *Proc. Inst. Mech. Eng. E J. Process. Mech. Eng.* **2022**, *237*, 410–417. [[CrossRef](#)]
34. Taha-Tijerina, J.; Shaji, S.; Kanakillam, S.S.; Mendivil-Palma, M.I.; Aviña, K. Tribological and Thermal Transport of Ag-Vegetable Nanofluids Prepared by Laser Ablation. *Appl. Sci.* **2020**, *10*, 1779. [[CrossRef](#)]
35. Akgul, Y.; Simsir, H. Anti-wear behaviour of silver nanoparticles on Al-Si alloy. *Surf. Topogr. Metrol. Prop.* **2021**, *9*, 025031. [[CrossRef](#)]
36. Duan, L.; Li, J.; Duan, H. Nanomaterials for lubricating oil application: A review. *Friction* **2022**, *11*, 647–684. [[CrossRef](#)]
37. Sarkar, S.; Ghosh, N.K. Effect of silver nanoparticle volume fraction on thermal conductivity, specific heat and viscosity of ethylene glycol base silver nanofluid: A molecular dynamics investigation. *J. Mol. Liq.* **2023**, *378*, 121635. [[CrossRef](#)]
38. Mirmohammadi, S.A.; Behi, M.; Gan, Y.; Shen, L. Particle-shape-, temperature-, and concentration-dependent thermal conductivity and viscosity of nanofluids. *Phys. Rev. E* **2019**, *99*, 043109. [[CrossRef](#)]
39. Meng, Y.; Su, F.; Chen, Y. Supercritical Fluid Synthesis and Tribological Applications of Silver Nanoparticle-decorated Graphene in Engine Oil Nanofluid. *Sci. Rep.* **2016**, *6*, 31246. [[CrossRef](#)]
40. Kumara, C.; Luo, H.; Leonard, D.N.; Meyer, H.M.; Qu, J. Organic-Modified Silver Nanoparticles as Lubricant Additives. *ACS Appl. Mater. Interfaces* **2017**, *9*, 37227–37237. [[CrossRef](#)]
41. Wang, J.; Zhuang, W.; Liang, W.; Yan, T.; Li, T.; Zhang, L. Inorganic nanomaterial lubricant additives for base fluids, to improve tribological performance: Recent developments. *Friction* **2022**, *10*, 645–676. [[CrossRef](#)]
42. Sunil, J.; Pooja, M.D.; Ginil, R.; Alex, S.N.; Pravin, A.A. Thermal conductivity and dynamic viscosity of aqueous-silver nanoparticle dispersion. *Mater. Today Proc.* **2021**, *37*, 122–124. [[CrossRef](#)]
43. Godson, L.; Raja, B.; Lal, D.M.; Wongwises, S. Experimental Investigation on the Thermal Conductivity and Viscosity of Silver-Deionized Water. *Nanofluids* **2010**, *23*, 317–332. [[CrossRef](#)]
44. Paul, G.; Sarkar, S.; Pal, T.; Das, P.K.; Manna, I. Concentration and size dependence of nano-silver dispersed water based nanofluids. *J. Colloid. Interface Sci.* **2012**, *371*, 20–27. [[CrossRef](#)] [[PubMed](#)]
45. Koca, H.D.; Doganay, S.; Turgut, A. Thermal characteristics and performance of Ag-water nanofluid: Application to natural circulation loops. *Energy Convers. Manag.* **2017**, *135*, 9–20. [[CrossRef](#)]
46. Aberoumand, S.; Jafarimoghaddam, A.; Aberoumand, H.; Javaherdeh, K. A Complete Experimental Investigation on The Rheological Behavior of Silver Oil Based Nanofluid. *Heat Transf. Res.* **2017**, *46*, 294–304. [[CrossRef](#)]
47. Khamliche, T.; Khamlich, S.; Doyle, T.B.; Makinde, D.; Maaza, M. Thermal conductivity enhancement of nano-silver particles dispersed ethylene glycol based nanofluids. *Mater. Res. Express* **2018**, *5*, 035020. [[CrossRef](#)]
48. Cárdenas-Contreras, E.M.; Oliveira, G.A.; Bandarra-Filho, E.P. Experimental analysis of the thermohydraulic performance of graphene and silver nanofluids in automotive cooling systems. *Int. J. Heat Mass Transf.* **2019**, *132*, 375–387. [[CrossRef](#)]
49. Flynn, J.H.; Wall, L.A. A quick, direct method for the determination of activation energy from thermogravimetric data. *J. Polym. Sci. Part B Polym. Lett.* **1966**, *4*, 323–328. [[CrossRef](#)]
50. Shafi, W.K.; Charoo, M.S. An overall review on the tribological, thermal and rheological properties of nanolubricants. *Tribol. Mater. Surf. Interfaces* **2020**, *15*, 20–54. [[CrossRef](#)]
51. Karthikeyan, K.M.B.; Vijayanand, J.; Arun, K.; Rao, V.S. Thermophysical and wear properties of eco-friendly nano lubricants. *Mater. Today Proc.* **2021**, *39*, 285–291. [[CrossRef](#)]
52. Smaisim, G.F.; Mohammed, D.B.; Abdulhadi, A.M.; Uktamov, K.F.; Alsultany, F.H.; Izzat, S.E. Nanofluids: Properties and applications. *J. Sol-Gel Sci. Technol.* **2022**, *104*, 1–35. [[CrossRef](#)]
53. Taha-Tijerina, J.; Aviña, K.; Martínez, J.M.; Arqueta-Guillén, P.Y.; González-Escobedo, M. Carbon Nanotube Structures for Thermal Transport Applications on Lubricants. *Nanomaterials* **2021**, *11*, 1158. [[CrossRef](#)] [[PubMed](#)]

Disclaimer/Publisher's Note: The statements, opinions and data contained in all publications are solely those of the individual author(s) and contributor(s) and not of MDPI and/or the editor(s). MDPI and/or the editor(s) disclaim responsibility for any injury to people or property resulting from any ideas, methods, instructions or products referred to in the content.